REVIEW

Clinical application of ultra-widefield fundus autofluorescence

Amin Xu · Changzheng Chen

Abstract

Purpose To review the basic principles of ultra-widefield fundus autofluorescence (UWF-FAF) and discuss its clinical application for a variety of retinal and choroidal disorders.

Methods A systematic review of the PubMed database was performed using the search terms "ultra-widefield," "autofluorescence," "retinal disease" and "choroidal disease."

Results UWF-FAF imaging is a recently developed noninvasive retinal imaging modality with a wide imaging range that can locate peripheral fundus lesions that traditional fundus autofluorescence cannot. Multiple commercially available ultra-widefield imaging systems, including Heidelberg Spectralis and Optomap Ultra-Widefield systems, are available to the clinician. Imaging by UWF-FAF is more comprehensive; it can reflect the content and distribution of the predominant ocular fluorophore in retinal pigment epithelial cells and evaluate the metabolic status of RPE of various retinal and choroidal disorders.

Conclusion UWF-FAF can detect abnormalities that traditional fundus autofluorescence cannot; therefore, it can be used to better elucidate disease pathogenesis,

analyze genotype–phenotype correlations, diagnose and monitor disease.

Background

Fundus autofluorescence (FAF) imaging is a noninvasive technology that can be used to detect the predominant ocular fundus fluorophores and naturally occurring molecules that absorb and emit light of specified wavelengths [1]. Since it was first reported by Delori in the 1980s, the application of FAF has enlarged in both practice and scope [1]. FAF imaging is particularly useful for assessing the types of diseases with modified RPE cells, including those with degenerative, dystrophic, inflammatory, infectious, neoplastic, and toxic etiologies. In addition, compared to the traditional fundus camera that is capable of acquiring 30° to 55° views of the posterior pole, ultra-widefield FAF (UWF-FAF) imaging allows visualization of peripheral ocular fundus lesions that FAF imaging is unable to detect (Fig. 1). Therefore, ultra-widefield (UWF) imaging is considered a supplementary optimal diagnostic method when evaluating the retina in its entirety. This review summarizes commonly used ocular fluorophores, various UWF-FAF imaging modalities, and the advantages and broad clinical

A. Xu · C. Chen (✉)
Department of Ophthalmology of Renmin Hospital of Wuhan University, No238, Jiefang Road, Wuhan 430060, Hubei, China
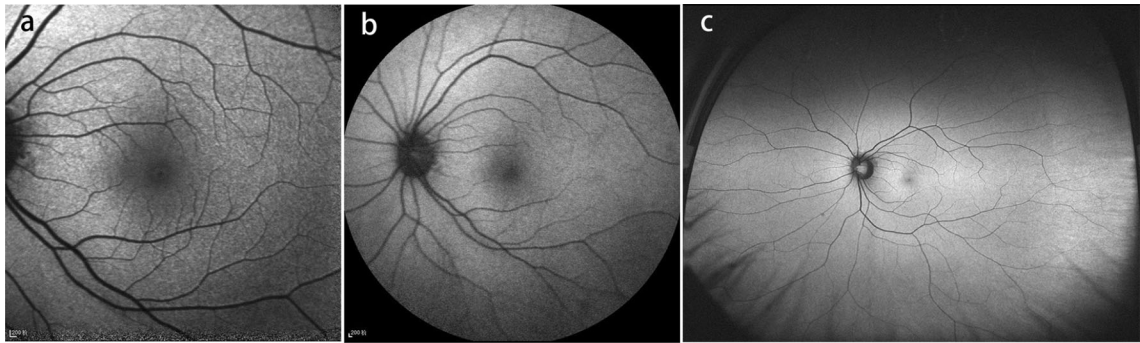e-mail: whuchenchzh@163.com

Fig. 1 Comparison of common imaging systems available for fundus autofluorescence. Images of healthy retina were obtained using the fundus camera with 30° (**a**), 55° (**b**), or 200° (**c**)

applications of UWF-FAF imaging and then highlights emerging research trends.

Generation of autofluorescence

Autofluorescence (AF) is a physical phenomenon, where, when certain substances are irradiated with specific wavelengths of light, they emit visible light over a very short period of time. Most substances in the eyeball can produce AF, and in order to produce AF, fluorophores absorb photons of the excitation wavelength, which elevates electrons to excited state. The electrons dispel some of this energy through molecular collisions and then emit a quantum of light at a lower energy and longer wavelength as they transit back to ground state. Generally speaking, FAF reflects the distribution of lipofuscin, and the predominant fluorophore located in the RPE.

The distribution of FAF in healthy human eyes has been characterized [2]. Both the optic nerve head and retinal vessels are hypofluorescent due to a lack of RPE cells and absorption of light by blood, respectively. The macula also has comparatively low levels of FAF due to increased zeaxanthin and lutein with accumulation being significantly lower in the fovea than in the temporal site. In the fovea, there is approximately 40% less fluorescence distributed in an asymmetric manner than at 7° eccentricity. The maximum fluorescence is located at approximately 11° temporally, 7° nasally, 13° superiorly, and 9° inferiorly. Compared to all other medians at the same eccentricity, AF is always the lowest along the inferior meridian. Lipofuscin AF increases linearly until 70 years of age and then declines [3]. The difference

observed between in vivo and ex vivo approximations of the rate of lipofuscin by RPE melanin accumulation may be due to the difference in absorption of light by RPE cells. The declining AF observed in old age may be a result of the removal of atrophic RPE cells. Lipofuscin is generally spatially distributed in a manner that maps with rods and is likely a reflection, rather than a prediction, of the pattern of rod photoreceptor loss with age. The following sections contain detailed descriptions of fluorescent substances in the ocular fundus.

Lipofuscin

Lipofuscin is found in postmitotic human RPE cells and accumulates as the age of the organism increases or cellular structural integrity is destroyed. Lipofuscin is the main fluorophore in human fundus, and it is created through the accumulation of metabolites from phagocytosis of the outer segment of photoreceptors by RPE cells [4]. Lipofuscin is primarily located in the posterior pole, and its level decreases toward the periphery [1, 5]. Previous studies have shown that N-retinyl-N-retinylidene ethanolamine (A2E) is the main component of lipofuscin and has an excitation wavelength of 430–450 nm and maximum emission wavelength of 560–575 nm [3]. A2E is a pyridium bisretinoid that accumulates in RPE lysosomes, where it exerts toxicity on the RPE cells and contributes to a variety of retinal degenerative diseases [6, 7]. Conversely, another study indicates A2E defends the retina from photooxidative damage [8]. However, A2E accumulation could be a sign of abnormal visual cycle activity, instead of retinal damage [8, 9]. A2E is mainly in the periphery of the retina, which is in

contrast to the posterior pole localization of lipofuscin, indicating that A2E may not be the fluorophore that increases macular FAF over time [10–12]. These results indicate that the role of A2E in retinal diseases is complicated and further studies are needed to fully detail its functions in this context.

Melanin

Melanin is an ocular pigment located in both RPE cells and uveal melanocytes. Unlike lipofuscin, melanin is distributed primarily in fovea, macula, and periphery [5]. Melanin granules are located apically in RPE cells compared to the basolateral location of lipofuscin [13, 14]. Melanin has a peak excitation that is the primary fluorophore in near-infrared AF at a longer wavelength of 787 nm [15]. However, on conventional FAF, melanin absorbs the short-wavelength excitation beam, decreasing the autofluorescent signal as a whole [3]. AF from melanin for 488 nm could be only 3–10% of the AF from lipofuscin, but it is unclear whether the secondary fluorophore detected in vivo during lipofuscin measurements was melanin [16].

Melanin protects eyes from diseases of ocular fundus [17]. Melanin located in anterior segment, such as the iris, can absorb and block visible light and ultraviolet radiation, thus preventing hypernomic light damage to the retina. Moreover, RPE cell melanin is an antioxidant and prevents the accumulation of free radicals, redox-reactive heavy metals, photooxidation, and lipofuscin [18–21]. However, this protective effect may decrease with age as melanin may become oxidized over time [22]. Notably, individuals with lightly pigmented irises and, thus, lower melanin levels in their RPE cells than individuals with darkly pigmented irises have a higher morbidity [23, 24].

Optic disk drusen

Optic disk drusen are the accumulation of extracellular autofluorescent mitochondria within the optic nerve head [25] and correlated with several ocular fundus diseases. As time passes, eyes with optic disk drusen may present with complications, such as visual field defects, optic nerve pallor, choroidal neovascularization, vascular occlusions, and hemorrhage [26].

Ultra-widefield fundus autofluorescence imaging systems

In recent years, UWF-FAF imaging has been used for clinical examination of the fundus and can acquire a fundus image covering 200° [27]. Therefore, this method expands the visual range of the ocular fundus and improves the clinical cognitive level of various fundus diseases. At present, commercially available UWF-FAF imaging devices include the Heidelberg Spectralis, noncontact UWF imaging, and the Optomap UWF system.

Heidelberg retinal angiography, which is now available as the Heidelberg Spectralis, is a scanning laser ophthalmoscope (SLO) that can use the excitation wavelength of blue light (488 nm) with a 500 nm barrier filter and offers a 102° noncontact lens attachment that can obtain about a 150° view of the retina. In addition, this technology can get infrared AF (815 nm) [28]. The Heidelberg Spectralis attaches to the camera head to provide high-contrast and evenly illuminate images of peripheral retina [29], and it can be easily exchanged with non-UWF lens. In addition, it can be used in conjunction with optical coherence tomography. However, this technique needs to dilate the pupils of patients and requires an experienced operator [30].

The Optomap UWF system can obtain a 200° view of the retina (about 82% of the retinal surface area) with a single image by combining confocal scanning laser technology with an ellipsoid mirror [31]. The advantage of an ellipsoidal mirror is that it has two focal points, one near the mirror and the other close to the pupillary plane. A point source of light emitted at the first focal point will thus converge within the patient's eye and permit a wide scanning angle even without pupillary dilation. The reflected or emitted light passes back through the confocal aperture and various filters including those necessary to detect fluorescence emission wavelengths (Fig. 2). The Optos system can use excitation wavelengths of green light (532 nm) with an emission filter of > 540 nm to visualize FAF. Green light excitation (532 nm) is superior to conventional blue light excitation (488 nm) for identifying the margins of lesion areas and for monitoring mild outer retinal damage [32]. It also has some additional benefits, including the ability to acquire images through an undilated pupil, a brief image acquisition time (250 ms), and a better
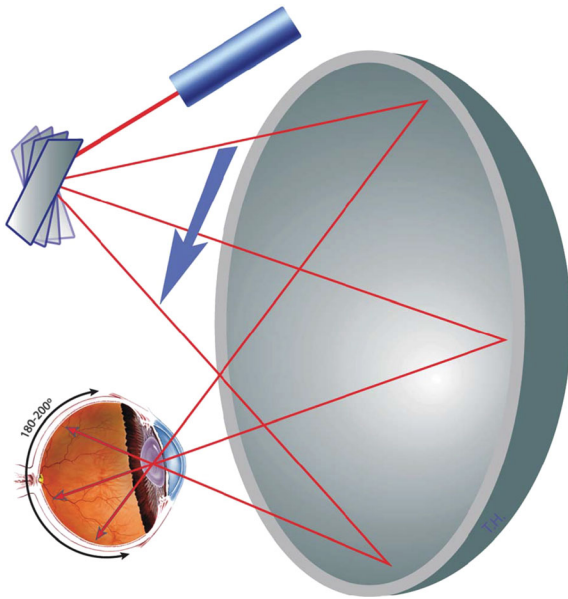
Fig. 2 Schematic illustration of ultra-widefield imaging of retina using an ellipsoidal mirror. A laser light source is reflected off the galvanometer mirrors onto an ellipsoidal mirror. The second focal point of the mirror resides within the eye, which facilitates image acquisition anterior to the equator. Photograph courtesy Nagiel et al. [67]

tolerance for a certain degree of ocular media opacity and smaller pupils. It can better evaluate the central and peripheral retina without rotating the eye. However, there are several limitations. Specifically, its imaging of the far superior and inferior peripheral retina is less complete than its imaging of the temporal and nasal retina [33], but this can be resolved by eye movement.

Ultra-widefield fundus autofluorescence imaging in clinical practice

UWF imaging offers great visualization of the retina with a single image, which allows simultaneous assessment of the AF levels in the macula and periphery and aids in obtaining more comprehensive and abundant information that was previously difficult to realize on the ocular fundus [27]. Below is a report on UWF-FAF studies of various ocular fundus diseases.

Age-related macular degeneration

Age-related macular degeneration (AMD) is a genetic and environmental disorder that leads to a slow decline of central vision. AMD may be related to vision loss independent of whether it is neovascular or nonneovascular [34]. In early non-neovascular AMD, FAF may show hyper- and hypo-autofluorescent areas that reveal more widespread disease than appreciated with color photography to evaluate the status of RPE, so FAF is a significant tool for evaluating the progression of AMD. Previously, studies were limited to the posterior pole [35, 36]. However, recent studies using UWF-FAF examined a group of AMD patients and found that AMD is often associated with peripheral AF changes in the retina [27, 37]. Witmer et al. [38] found that 63.6% of eyes with AMD had peripheral abnormalities in AF. Similar studies found that 68.9% of AMD patients had abnormal peripheral AF that can be categorized into three types: granular, mottled, and nummular (Fig. 3) [39]. There is a high correlation between specific FAF and clinical findings for granular fluorescence with peripheral drusen and mottled fluorescence with RPE depigmentation [39]. Another study found five types of peripheral AF: normal, focal pinpoint, granular, patchy, and reticular [38]. When changes in granular fluorescence were assessed, it was found patchy hypofluorescence is more common in eyes with advanced-stage AMD than in eyes with early-stage AMD [38]. In addition, changes in granular fluorescence are also more common in eyes with choroidal neovascularization or geographic atrophy, while patchy hypofluorescence is more common in eyes with geographic atrophy [38]. The researchers believe that peripheral abnormal fluorescence is typically present in AMD patients, and different peripheral findings in eyes with AMD may represent different types of AMD and indicate the development of AMD is associated with different environmental and genetic factors [38]. Furthermore, the Age-Related Eye Disease Study pointed out that abnormal changes in AF in the periphery of the retina are more common in eyes with AMD than in control eyes. In the majority of eyes with AMD, drusen are present not only at the posterior pole, but also in the far periphery. Therefore, the authors stated AMD may not just concern the "macular" area, but, rather, the whole retina [40, 41]. UWF-FAF may be useful for evaluating wider retinal dysfunction [42]. Furthermore,
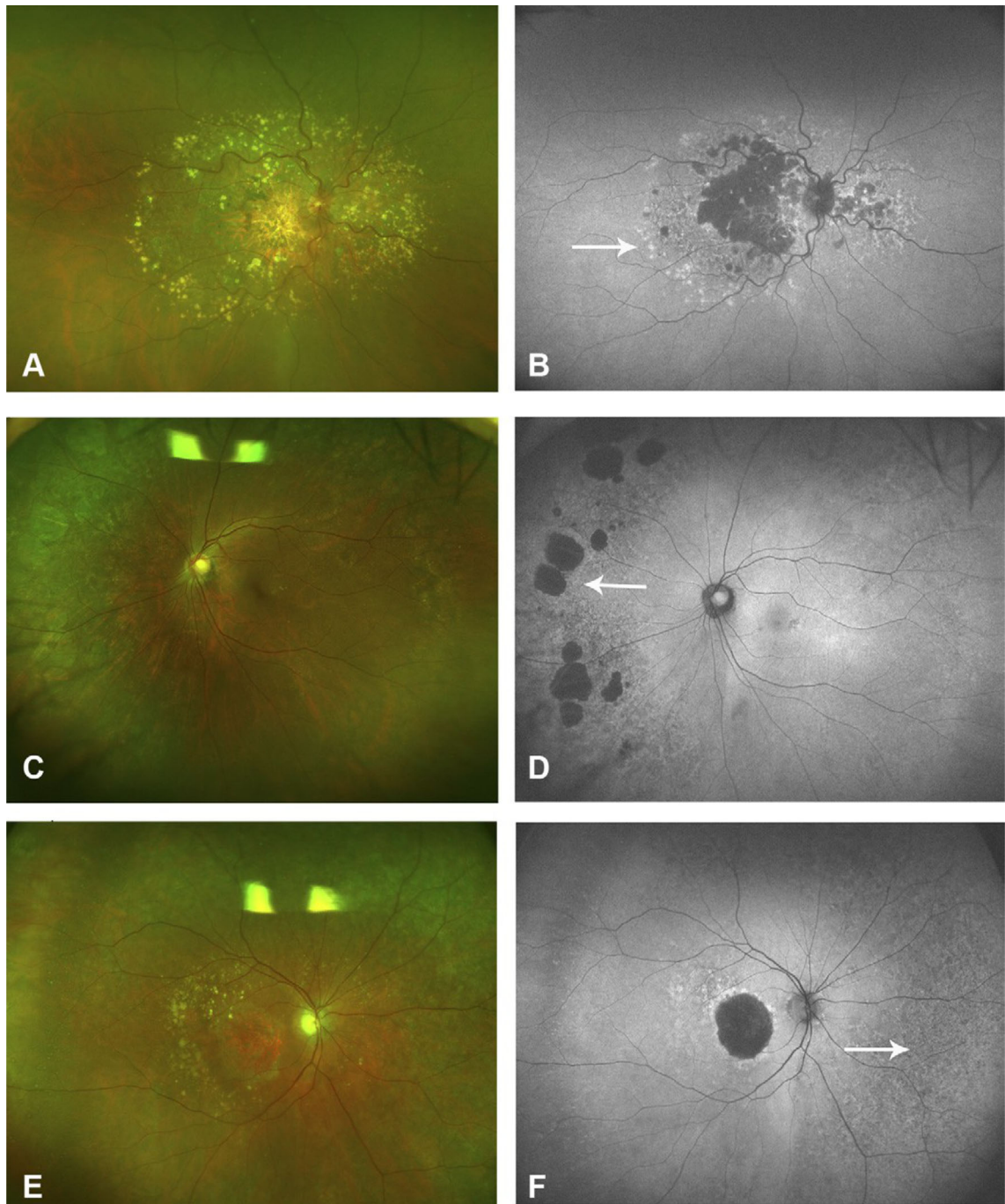
Fig. 3 Color and autofluorescence photographs illustrating FAF abnormalities and the associated clinical features. **a** Color fundus photography illustrating peripheral drusen. **b** FAF image showing granular increased autofluorescence corresponding to the drusen (white arrow). **c** Areas of retinal pigment epithelium (RPE) atrophy in the nasal periphery. **d** FAF image showing the nummular areas with decreased autofluorescence (white arrow) corresponding to the RPE atrophy. **e** Areas of RPE depigmentation in the periphery of the fundus. Small peripheral drusen are seen temporally. **f** FAF image demonstrating the large mottled areas with decreased autofluorescence (white arrow) corresponding to the area of RPE depigmentation. Fine granular FAF is also seen temporally corresponding to peripheral drusen. Photograph courtesy Tan et al. [39]

Klufas et al. [43] found that UWF indocyanine green angiography combined with UWF fluorescein angiography and UWF-FAF allows better observation and interpretation of changes in the peripheral retina in AMD eyes. This is important for evaluating the progress of choroidal retinopathy. However, at present, there are few longitudinal studies on AMD using UWF-FAF. In the future, a large sample longitudinal study will be needed to enhance the clinician's understanding of the pathogenesis and progression of AMD.

Central serous chorioretinopathy

Central serous chorioretinopathy (CSC) is a disease of serous retinal detachment (SRD) associated with leakage of fluid through the RPE into the subretinal space [44]. Patients can experience the loss of visual acuity and central dark spots and metamorphopsia. FAF enables an adequate assessment of RPE metabolic activity by measuring its content of lipofuscin and may even predict visual acuity. FAF image shows focal hyperautofluorescence corresponding with focal RPE detachment. As the disease progresses, it can show other autofluorescence, such as granular hyperautofluorescence corresponding to subretinal precipitates on OCT (Fig. 4a, b) [45]. Previously, studies on CSC using FAF only evaluated the posterior pole with a 50° range [46]. One such study found that 57% of CSC patients had widespread involvement of the peripheral retina [47]. The hyperautofluorescent precipitates gravitate inferiorly or collect at the borders of the detachment. In chronic CSC, it can show hypoautofluorescent atrophic gravitational tracts in the periphery that correlate with prior dependent subretinal fluid (Fig. 4c). Compared with conventional confocal SLO, UWF-FAF can more comprehensively monitor subretinal conditions in eyes with SRD and more accurately evaluate mild outer retinal status in eyes without SRD [32]. CSC is traditionally thought to be a disease involving macular areas. However, since it often involves the peripheral retina, Pang et al. [47] pointed out that UWF-FAF combined with indocyanine green angiography in CSC could reveal more extensive disease with a single image than with conventional standard field imaging and may be helpful for monitoring SRF, choroidal hyper-permeability, recurrent disease, and treatment for active disease. However, at present, the studies on using UWF-FAF for
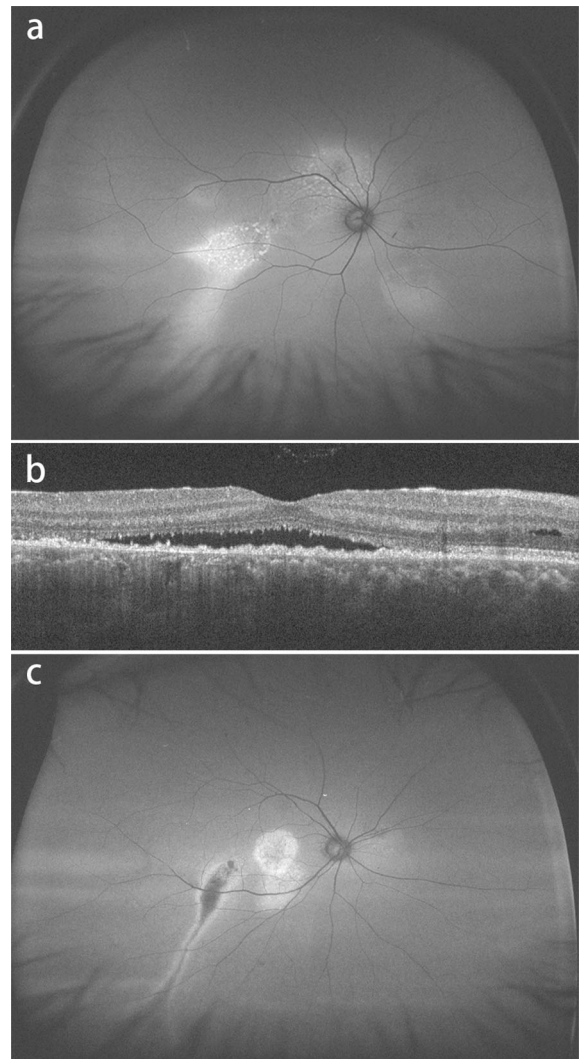
Fig. 4 UWF-FAF of central serous chorioretinopathy. **a** FAF shows granular hyperautofluorescence corresponding to subretinal precipitates on SD-OCT. **b** SD-OCT of the lesion shows a serous retinal detachment associated with subretinal precipitates. **c** FAF shows granular hyperautofluorescence in the macular and hypoautofluorescent atrophic gravitational tracts in the periphery

CSC are mostly cross-sectional, which fail to provide information on patient condition over time. In the future, more longitudinal studies are needed to better evaluate the prognosis of CSC patients.

Uveitis

Uveitis with or without an underlying systematic disease is classified anatomically into anterior,

intermediate, or posterior according to the primary site of inflammation. The posterior form has a very heterogeneous clinical presentation and can include focal, multifocal, or diffuse choroiditis, chorioretinitis, retinitis, and/or neuroretinitis. It is difficult to comprehensively assess peripheral fundus lesions as the traditional camera is not conducive to objectively and accurately evaluate the range of motion and the extent of uveitis owing to a small imaging range. By contrast, noninvasive UWF-FAF detects more retinal or chorioretinal involvement in patients with posterior uveitis than color imaging [48]. Similarly, Heussen et al. [49] found that 70% of patients with Vogt–Koyanagi–Harada had abnormal changes in AF in the peripheral retina that could be divided into three different patterns: multifocal hypofluorescent spots, hyperfluorescent spots, and a unique lattice-like pattern. The findings of this study also suggest that active retinal vasculitis in patients with Behcet's disease may induce alterations in the retinal epithelium in the retinal periphery. These abnormalities were visible with UWF-FAF imaging and present as multiple hyperfluorescent spots in the retinal periphery [50].

It is difficult to identify the affected lesions in multiple evanescent white dot syndrome (MEWDS) because of faint and transient white dots in the peripheral fundus and diffuse faint retinal opacities in the posterior fundus. Now we can use UWF-FAF technology to investigate the evolution of the affected lesions in acute MEWDS. Researchers have observed that the lesions in MEWDS originate from the optic disk and the posterior pole during the acute period, spread in a centrifugal manner to the periphery, and then eventually fade away from the periphery in a centripetal manner [51]. On FAF, the multifocal lesions have increased signal strength due to photoreceptor loss and unmasking of natural RPE autofluorescence (Fig. 5). Furthermore, Seidensticker et al. [52] found UWF-FAF imaging can detect visual field defect-related changes in RPE cells in chorioretinitis patients. Through these studies, it can be concluded that abnormal fluorescence of the peripheral retina is common in uveitis. The evaluation of UWF-FAF can reveal more information about patients with uveitis and help to confirm the type of uveitis. In addition, UWF-FAF imaging can aid in understanding the evolution of the disease and diagnosing and following up with patients with posterior uveitis. At present,

further studies are needed to determine how the new findings concerning the peripheral retina relate to different types of uveitis and how treatment changes the prognosis of patients with uveitis.

Inherited retinal dystrophies

Inherited retinal dystrophy (IRD) is a heterogeneous group of disorders affecting photoreceptors [53]. Reduced AF is thought to result from photoreceptor loss in early life and occur with RPE loss, while enhanced AF is from increased lipofuscin in RPE cells or the loss of outer segments of rods [54]. FAF is a viable imaging modality to monitor IRD and correlate phenotype with genotype [55]. UWF-FAF imaging provides a 200° view of the retina in a single imaging [27], allowing simultaneous visualization of macular and peripheral AF. With wide-field analysis, more peripheral fundus lesions can be found and abnormal FAF areas may be able to be associated with visual function in retinitis pigmentosa (RP) and cone-rod dystrophy [53, 56]. Furthermore, the presence of patchy hypoautofluorescence on UWF-FAF was reliably related to patient age, duration of symptoms, and visual acuity [53]. Similarly, this study indicated areas of hypoautofluorescence on FAF images correlate significantly with the areas with visual field defects [55]. Another study stated that the extent of FAF abnormalities reflects the severity of functional impairment in patients with cone dominant retinal dystrophies [57]. In addition, this research group was able to estimate the visual field in RP patients using the objective measurements from UWF-FAF imaging and hypothesized the presence of patchy hypofluorescent lesions can be used as an indicator for the duration of RP [58]. Trichonas et al. explored possible correlations between genotype and UWF-FAF patterns in patients with RP and retinal dystrophies and found that UWF-FAF provides important information that helps diagnosis. Further studies are needed to better apply this technology as an imaging biomarker to identify genetic relationships in RP and retinal dystrophies [59].

The majority of cases of Stargardt disease (STGD) are caused by autosomal recessive mutations in ABCA4 [60]. Mutations in ABCA4 may also give rise to correlating disorders, such as autosomal recessive RP, cone-rod dystrophy [61], or AMD [62]. In a recent study, a new UWF-FAF classification
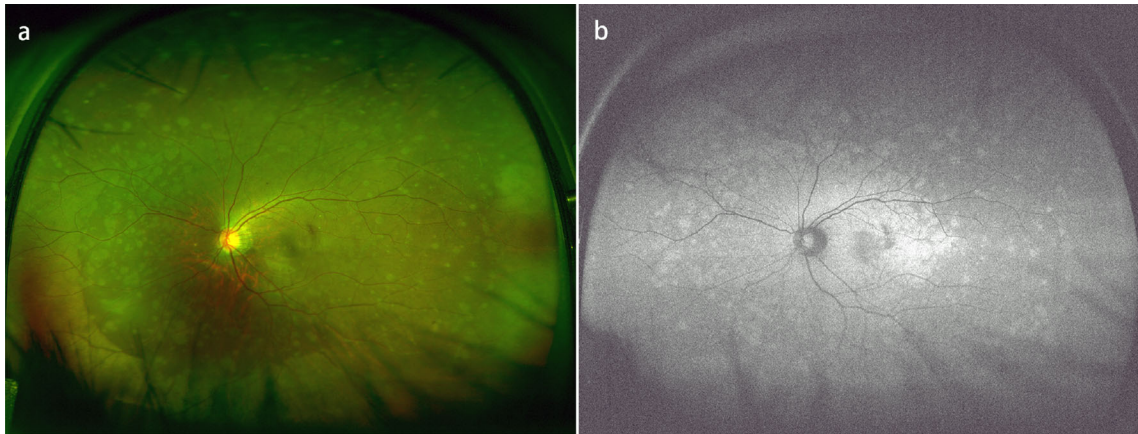
Fig. 5 A 45-year-old female patient has multiple evanescent white dot syndrome in her left eye. **a** A color fundus photograph shows foveal granularity and scattered yellowish spots in the posterior pole and nasal midperiphery. **b** UWF-FAF image shows diffuse hyperautofluorescence in the peripapillary retina and posterior pole and numerous hyperautofluorescent spots in the periphery

system of ABCA4 in STGD consisting of three patterns of Type I, Type II, and Type III has been described and implemented (Table 1) [63]. Despite the classic early changes of STGD being limited to the macular with this heritable disorder, generalized retinal dysfunction is clearly a feature of some, if not all, forms of STGD [64]. The first series of UWF imaging on STGD patients confirmed ABCA4 genotypes, and a review of the UWF-FAF images in this study revealed abnormalities in the peripheral retina are present in the vast majority of cases and would otherwise be missed by conventional FAF imaging [63]. Patients with widespread disease presented with more constriction of peripheral visual fields and had more dysfunction on full-field electroretinogram

and worse visual acuity compared to patients with disease confined to the macula [65]. And the effective radius growth rate of atrophic lesions could serve as a reliable outcome measure to monitor STGD progression [66]. UWF-FAF images may provide information for estimating peripheral and central visual function in STGD. However, due to the complexity of the ABCA4 locus and the large number of mutations/variants, correlating UWF-FAF phenotypes with ABCA4 genotypes remains a challenge.

Through the research described above, although most abnormalities occur in the macular area, they later accumulate in the periphery. The association between UWF-FAF, visual field deficits, and even visual acuity portends a future in which multimodal

Table 1 UWF-FAF Patterns in Stargardt disease

Classification with UWF-FAF	
Type I	Central atrophy with or without flecks confined to posterior pole—No findings outside 55° field of view
Type II	Central atrophy with flecks only extending outside posterior pole
Type III	Central atrophy and significant extramacular flecks and atrophy extending outside posterior pole

	Subtypes
	A: mild/moderate atrophy (most often in punctate pattern) extending to or beyond equator
	B: severe atrophy extending from macula to equator
	C: extensive, severe atrophy extending anterior to equator

UWF testing will become standard-of-care for the management of these patients. It is possible that testing will shift away from visual fields and move toward more objective measures of disease progression, such as total area or pattern of AF changes [67]. Furthermore, the full clinical significance of the UWF-FAF findings for IRD, especially in relation to correlations between genotype and phenotype, will require prospective longitudinal studies with improved genotyping technologies. UWF-FAF imaging will allow clinicians to better assess peripheral photoreceptor and RPE layer information and monitor the progress of disease in IRD patients.

Tumors

Choroidal melanoma

Choroidal melanoma (CM) is the most common primary malignancy of the eye [68]. Fortunately, the incidence of CM is relatively low. By contrast, benign melanocytic choroidal nevi are common, occurring in 2–5% of the US population [69]. Biomicroscopy, together with fundus photography and ultrasound echography, is the most commonly used technology to diagnose and monitor choroidal lesions. But these techniques are of lower diagnostic value when differentiating benign and malignant pigmented lesions of the ocular fundus, especially for smaller lesions. Optomap Panoramic 200Tx images offer two types of laser scans and additional UWF-FAF detection to differentiate nonmalignant from malignant choroidal lesions [70]. The mean FAF intensity of melanomas is significantly lower than in choroidal nevi. In addition, when using "green laser separation," melanomas trend toward a more mixed FAF appearance compared to nevi. The mean maximal and minimal transverse and longitudinal diameters of melanomas are also significantly higher than those of nevi [71]. It has been demonstrated that wide-field SLO imaging and FAF imaging are noninvasive diagnostic screening tools suitable for distinguishing benign from malign pigmented choroidal lesions [71].

Optic disk melanocytoma

Optic disk melanocytoma (ODM) is a benign tumor typically occurring on or near the optic disk [72]. Clinically, these tumors are categorized into juxtapapillary uveal melanoma (JUM), juxtapapillary choroidal nevus (JCN), hyperplasia of the retinal pigment epithelium, hypertrophy of the retinal pigment epithelium, combined hamartoma of the retina and RPE layer, or adenoma of the RPE layer [73]. FAF imaging can evaluate the lipofuscin content in RPE cells [74]. Furthermore, the distribution and intensity of FAF may help clarify pathophysiological mechanisms [75]. The fluorescence properties are often altered in intraocular malignancy, and it is very important sign for JUM to detect orange pigment [76]. Upon UWF-FAF examination, ODM presents as an entirely hypofluorescent mass with clearly demarcated, feathery edges with no hyperfluorescent changes due to existing orange pigment or subretinal fluid (Fig. 6) [77]. However, JCN and JUM present with either focal hyperfluorescence or massive hyperfluorescent areas at the tumor and its boundary [77]. Therefore, it is thought that UWF-FAF imaging is an appropriate noninvasive tool for differential diagnosis of ODM based on its lack of hyperfluorescence compared to JCN and JUM [77].

Vitrectomy surgery

Macular hole

A macular hole (MH) is a retinal hole in the macular area that can cause a serious decrease in visual function. The advent of vitrectomy surgery and the development of surgical techniques have improved the vision of these patients [78]. Studies have indicated that OCT can monitor the closure of MH through the air bubble in patients with a gas-filled eye [79]. However, existing fundus examination techniques of evaluating the retina, such as OCT, are unable to obtain clear fundus images in gas-filled eyes. FAF imaging is a new way by which to evaluate MH surgical outcomes [80, 81], where MH may disappear after successful surgical repair [81]. An increased intensity of an autofluorescence spot in the macula is consistent with a loss of foveal tissue, especially in a complete full-thickness MH [80]. FAF disappearance from the MH may occur after successful surgical repair [81]. Quantitative analysis of UWF-FAF images can reveal complete or partial closure of MHs in gas-filled eyes after surgery [82]. However, autofluorescent imaging of the macular area could also be disturbed by the gas–water interface in the
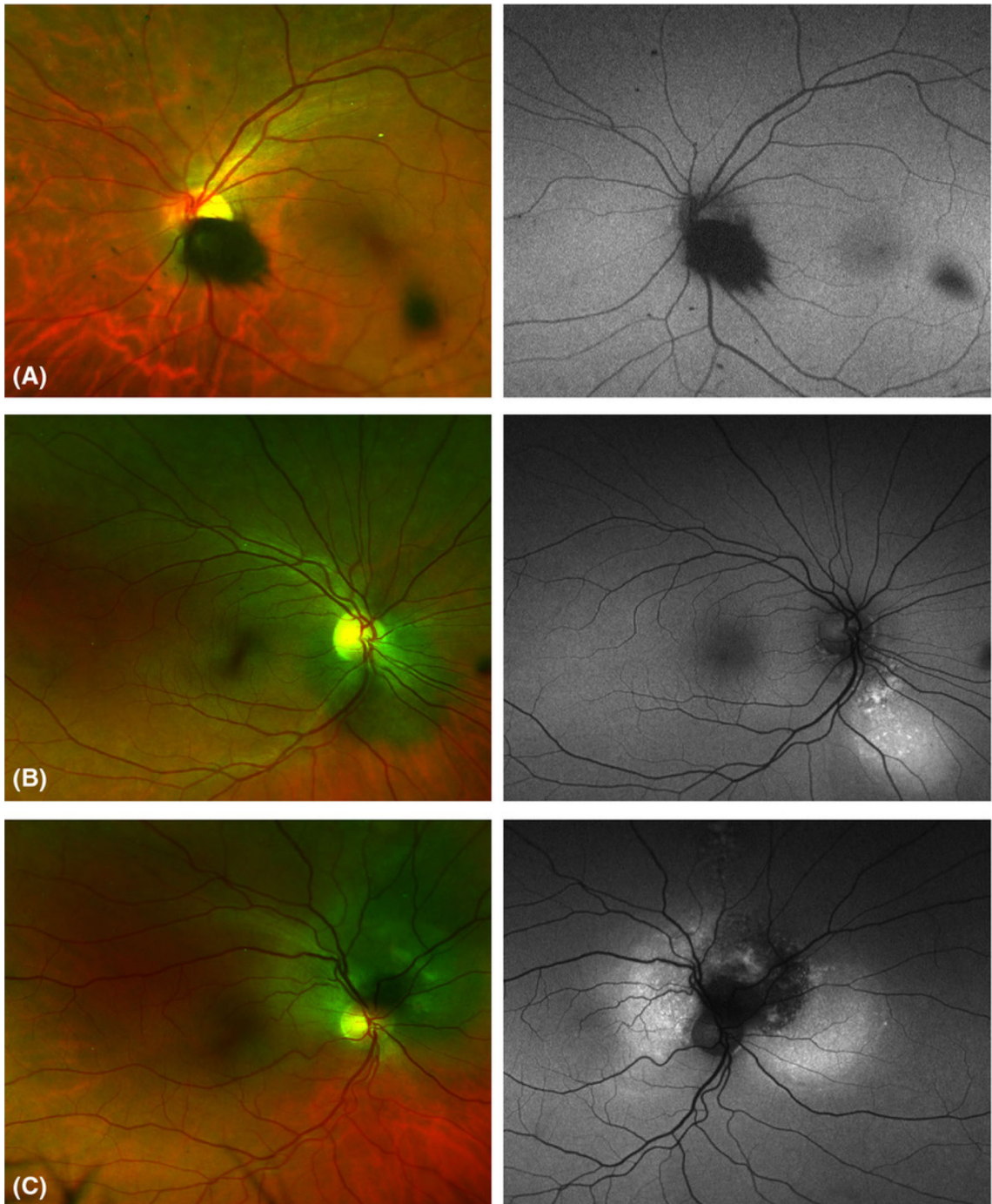
Fig. 6 **a** Color and FAF images of optic disk melanocytoma (ODM). Notice the well-demarcated, feathery edges in both color and FAF images, as well as the absence of pathologic hyperfluorescence. **b** Color and FAF images of juxtapapillary choroidal nevus (JCN). Notice several focal hyperfluorescent areas inside the tumor area, and the larger hyperfluorescent space due to subretinal fluid, obscuring the tumor margins and significantly increasing the risk of tumor growth in this asymptomatic patient. **c** Color and FAF images of juxtapapillary uveal melanoma (JUM). Notice the focal hyperfluorescence from orange pigment in the tumor area and the hyperfluorescence from subretinal fluid leakage on and around the tumor. Photograph courtesy Salvanos et al. [77]

vitrectomy [82]. Changing the orientation of the patient's face or eye fixation may improve the quality of FAF imaging [82]. Therefore, UWF-FAF imaging may be a useful tool for surgeons to use when assessing visual function after vitrectomy surgery of MHs [82].

Rhegmatogenous retinal detachment

Rhegmatogenous retinal detachment (RRD) is the separation of the neurosensory retina from the RPE layer because of a retinal hole [83]. There are several causes of decreased visual acuity after successful repair of retinal detachment, including persistent foveal detachment [84], epiretinal membrane, and cystoid macular edema [85]. But the nutrition of the photoreceptor layer may be impaired after RRD. It is difficult to monitor retinal function even after successful surgery. FAF imaging can be used to evaluate the functional status of the retina. Using UWF-FAF imaging, Witmer et al. [86] found that the area of retinal detachment is hypofluorescent. A hypofluorescent leading edge (HLE) to the retinal detachment was observed preoperatively in most of eyes [86] (Fig. 7). In all patients with a HLE preoperatively, the HLE resolved by the one-month postoperative visit. In addition, 44% of the eyes with the macular area involved before surgery contained granular fluorescence after surgery [86]. Therefore, UWF-FAF

imaging can detect abnormalities in RRD and assist in preoperative characterization of detachment and postoperative assessment [86]. Another study found light and moderate cryopexy induce hyperfluorescence of the treated area that leads to central hypofluorescence with a hyperfluorescent halo. However, extensive cryopexy and disruption of the RPE layer led to a broad hypofluorescent area with hyperfluorescent areas, including demarcation lines and vestigial subretinal fluid [87]. UWF-FAF can reveal dynamic changes at the peripheral retina beyond the vascular arcades. UWF-FAF imaging that provides a surgeon with a greater appreciation of the extent of the retinal detachment preoperatively, unlike pseudocolor imaging, is capable of detecting and monitoring lesion area. It may be not only helpful in more extensively evaluating retinal dysfunction, but also useful for longitudinal assessments in natural history studies [42]. However, at present, the research on UWF-FAF in the context of RRD is limited with related studies having small sample sizes and short follow-up periods. In the future, large sample-sized prospective studies are needed to observe the recovery of retinal function in RRD patients during long-term follow-up.
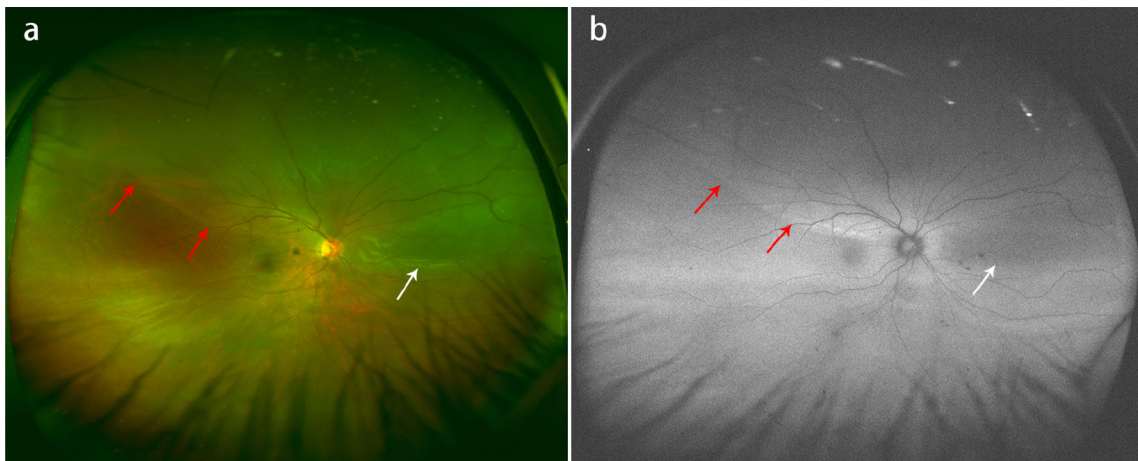

Fig. 7 a Preoperative UWF color image of retinal detachment without involving the fovea. The white arrow identifies the area of bullous retinal detachment. The red arrow identifies an area of shallow neurosensory detachment extending through the fovea. **b** Preoperative UWF-FAF image of the same patient demonstrating the area of bullous detachment as hypofluorescence (white arrow) and the HLE marked with red arrow, indicating the area of shallow neurosensory detachment

Future directions

UWF-FAF technology has become important clinically with regard to monitoring most sight-threatening retinal diseases. However, questions about UWF-FAF examination remain. The enlargement of the fundus imaging range may sacrifice image resolution and even distort the surrounding image, leading to inaccurate measurements of the actual location and size of the lesion. In addition, patients with eyelashes and ocular media opacity are prone to form artifacts, resulting in reduced image readability. Although Singer et al. [88] used the montage function to perform stereoscopic projection for different eye position images, which automatically realized the image localization and solved the distortion issues in the peripheral retina image. However, this function is not currently widely used. Of course, in addition to the further improvements required to solve these technical issues in this equipment, it is important that clinicians and researchers using UWF systems for FAF imaging are aware of the limitations of the method and receive adequate training in how to make full use of the equipment in a standardized manner and reasonably interpret the resulting FAF images. Nevertheless, as a noninvasive examination tool, UWF-FAF has attracted increasing attention with its use in the diagnosis, treatment, and follow-up of ocular disease being research hot spots. In the future, this technology will continue to evolve and promote clinical and scientific research of ocular fundus diseases.

Conclusion

FAF provides information on the metabolic state and overall health of the RPE layer, and indirectly, the photoreceptor layer. UWF imaging allows for improved detection and analysis of many pathologic retinal conditions with peripheral findings. In the future, UWF-FAF imaging will undoubtedly include even wider clinical applications and newly discovered capabilities that will extend its diagnostic power. An important task for future investigation is to elucidate the clinical significance of pathology in the far periphery and how it informs management decisions.

References

1. Delori FC, Dorey CK, Staurenghi G, Arend O, Goger DG, Weiter JJ (1995) In vivo fluorescence of the ocular fundus exhibits retinal pigment epithelium lipofuscin characteristics. Invest Ophthalmol Vis Sci 36:718–729
2. von Ruckmann A, Fitzke FW, Bird AC (1995) Distribution of fundus autofluorescence with a scanning laser ophthalmoscope. Br J Ophthalmol 79:407–412
3. Delori FC, Goger DG, Dorey CK (2001) Age-related accumulation and spatial distribution of lipofuscin in RPE of normal subjects. Invest Ophthalmol Vis Sci 42:1855–1866
4. Spital G, Radermacher M, Muller C, Brumm G, Lommatzsch A, Pauleikhoff D (1998) Autofluorescence characteristics of lipofuscin components in different forms of late senile macular degeneration. Klin Monbl Augenheilkd 213:23–31
5. Weiter JJ, Delori FC, Wing GL, Fitch KA (1986) Retinal pigment epithelial lipofuscin and melanin and choroidal melanin in human eyes. Invest Ophthalmol Vis Sci 27:145–152
6. Schutt F, Davies S, Kopitz J, Holz FG, Boulton ME (2000) Photodamage to human RPE cells by A2-E, a retinoid component of lipofuscin. Invest Ophthalmol Vis Sci 41:2303–2308
7. Bergmann M, Schutt F, Holz FG, Kopitz J (2004) Inhibition of the ATP-driven proton pump in RPE lysosomes by the major lipofuscin fluorophore A2-E may contribute to the pathogenesis of age-related macular degeneration. FASEB J 18:562–564
8. Maeda A, Golczak M, Chen Y, Okano K, Kohno H, Shiose S, Ishikawa K, Harte W, Palczewska G, Maeda T, Palczewski K (2011) Primary amines protect against retinal degeneration in mouse models of retinopathies. Nat Chem Biol 8:170–178
9. Roberts JE, Kukielczak BM, Hu DN, Miller DS, Bilski P, Sik RH, Motten AG, Chignell CF (2002) The role of A2E in prevention or enhancement of light damage in human retinal pigment epithelial cells. Photochem Photobiol 75:184–190

10. Crouch RK, Koutalos Y, Kono M, Schey K, Ablonczy Z (2015) A2E and lipofuscin. Prog Mol Biol Transl Sci 134:449–463

11. Ablonczy Z, Higbee D, Anderson DM, Dahrouj M, Grey AC, Gutierrez D, Koutalos Y, Schey KL, Hanneken A, Crouch RK (2013) Lack of correlation between the spatial distribution of A2E and lipofuscin fluorescence in the human retinal pigment epithelium. Invest Ophthalmol Vis Sci 54:5535–5542

12. Smith RT, Bernstein PS, Curcio CA (2013) Rethinking A2E. Invest Ophthalmol Vis Sci 54:5543

13. Feeney L (1978) Lipofuscin and melanin of human retinal pigment epithelium. Fluorescence, enzyme cytochemical, and ultrastructural studies. Invest Ophthalmol Vis Sci 17:583–600

14. Feeney-Burns L, Hilderbrand ES, Eldridge S (1984) Aging human RPE: morphometric analysis of macular, equatorial, and peripheral cells. Invest Ophthalmol Vis Sci 25:195–200

15. Keilhauer CN, Delori FC (2006) Near-infrared autofluorescence imaging of the fundus: visualization of ocular melanin. Invest Ophthalmol Vis Sci 47:3556–3564

16. Kayatz P, Thumann G, Luther TT, Jordan JF, Bartz-Schmidt KU, Esser PJ, Schraermeyer U (2001) Oxidation causes melanin fluorescence. Invest Ophthalmol Vis Sci 42:241–246

17. Hu DN, Simon JD, Sarna T (2008) Role of ocular melanin in ophthalmic physiology and pathology. Photochem Photobiol 84:639–644

18. Burke JM, Kaczara P, Skumatz CM, Zareba M, Raciti MW, Sarna T (2011) Dynamic analyses reveal cytoprotection by RPE melanosomes against non-photic stress. Mol Vis 17:2864–2877

19. Wang Z, Dillon J, Gaillard ER (2006) Antioxidant properties of melanin in retinal pigment epithelial cells. Photochem Photobiol 82:474–479

20. Rozanowski B, Burke JM, Boulton ME, Sarna T, Rozanowska M (2008) Human RPE melanosomes protect from photosensitized and iron-mediated oxidation but become pro-oxidant in the presence of iron upon photodegradation. Invest Ophthalmol Vis Sci 49:2838–2847

21. Sundelin SP, Nilsson SE, Brunk UT (2001) Lipofuscin-formation in cultured retinal pigment epithelial cells is related to their melanin content. Free Radic Biol Med 30:74–81

22. Sarna T (1992) Properties and function of the ocular melanin–a photobiophysical view. J Photochem Photobiol B 12:215–258

23. Nicolas CM, Robman LD, Tikellis G, Dimitrov PN, Dowrick A, Guymer RH, McCarty CA (2003) Iris colour, ethnic origin and progression of age-related macular degeneration. Clin Exp Ophthalmol 31:465–469

24. Weiter JJ, Delori FC, Wing GL, Fitch KA (1985) Relationship of senile macular degeneration to ocular pigmentation. Am J Ophthalmol 99:185–187

25. Tso MO (1981) Pathology and pathogenesis of drusen of the optic nervehead. Ophthalmology 88:1066–1080

26. Friedman AH, Beckerman B, Gold DH, Walsh JB, Gartner S (1977) Drusen of the optic disc. Surv Ophthalmol 21:373–390

27. Heussen FM, Tan CS, Sadda SR (2012) Prevalence of peripheral abnormalities on ultra-widefield greenlight

28. Ben Moussa N, Georges A, Capuano V, Merle B, Souied EH, Querques G (2015) MultiColor imaging in the evaluation of geographic atrophy due to age-related macular degeneration. Br J Ophthalmol 99:842–847

29. Witmer MT, Parlitsis G, Patel S, Kiss S (2013) Comparison of ultra-widefield fluorescein angiography with the Heidelberg Spectralis((R)) noncontact ultra-widefield module versus the Optos((R)) Optomap((R)). Clin Ophthalmol 7:389–394

30. Staurenghi G, Viola F, Mainster MA, Graham RD, Harrington PG (2005) Scanning laser ophthalmoscopy and angiography with a wide-field contact lens system. Arch Ophthalmol 123:244–252

31. Cicinelli MV, Cavalleri M, Brambati M, Lattanzio R, Bandello F (2019) New imaging systems in diabetic retinopathy. Acta Diabetol. https://doi.org/10.1007/s00592-019-01373-y

32. Shin JY, Choi HJ, Lee J, Choi M, Chung B, Byeon SH (2016) Fundus autofluorescence findings in central serous chorioretinopathy using two different confocal scanning laser ophthalmoscopes: correlation with functional and structural status. Graefes Arch Clin Exp Ophthalmol 254:1537–1544

33. Bonnay G, Nguyen F, Meunier I, Ducasse A, Hamel C, Arndt C (2011) Screening for retinal detachment using wide-field retinal imaging. J Fr Ophtalmol 34:482–485

34. Klein R, Chou CF, Klein BE, Zhang X, Meuer SM, Saaddine JB (2011) Prevalence of age-related macular degeneration in the US population. Arch Ophthalmol 129:75–80

35. Holz FG, Bellman C, Staudt S, Schutt F, Volcker HE (2001) Fundus autofluorescence and development of geographic atrophy in age-related macular degeneration. Invest Ophthalmol Vis Sci 42:1051–1056

36. Sepah YJ, Akhtar A, Sadiq MA, Hafeez Y, Nasir H, Perez B, Mawji N, Dean DJ, Ferraz D, Nguyen QD (2014) Fundus autofluorescence imaging: fundamentals and clinical relevance. Saudi J Ophthalmol 28:111–116

37. Nomura Y, Takahashi H, Tan X, Obata R, Yanagi Y (2015) Widespread choroidal thickening and abnormal midperipheral fundus autofluorescence characterize exudative age-related macular degeneration with choroidal vascular hyperpermeability. Clin Ophthalmol 9:297–304

38. Witmer MT, Kozbial A, Daniel S, Kiss S (2012) Peripheral autofluorescence findings in age-related macular degeneration. Acta Ophthalmol 90:e428–e433

39. Tan CS, Heussen F, Sadda SR (2013) Peripheral autofluorescence and clinical findings in neovascular and non-neovascular age-related macular degeneration. Ophthalmology 120:1271–1277

40. Writing Committee for the OPRs, Domalpally A, Clemons TE, Danis RP, Sadda SR, Cukras CA, Toth CA, Friberg TR, Chew EY (2017) Peripheral retinal changes associated with age-related macular degeneration in the age-related eye disease study 2: age-related eye disease study 2 report number 12 by the age-related eye disease study 2 optos peripheral retina (OPERA) study research group. Ophthalmology 124:479–487

41. Forshaw TRJ, Minor AS, Subhi Y, Sorensen TL (2019) Peripheral retinal lesions in eyes with age-related macular

degeneration using ultra-widefield imaging: a systematic review with meta-analyses. Ophthalmol Retina. https://doi.org/10.1016/j.oret.2019.04.014

42. Duisdieker V, Fleckenstein M, Zilkens KM, Steinberg JS, Holz FG, Schmitz-Valckenberg S (2015) Long-term follow-up of fundus autofluorescence imaging using wide-field scanning laser ophthalmoscopy. Ophthalmologica 234:218–226

43. Klufas MA, Yannuzzi NA, Pang CE, Srinivas S, Sadda SR, Freund KB, Kiss S (2015) Feasibility and clinical utility of ultra-widefield indocyanine green angiography. Retina 35:508–520

44. Nicholson B, Noble J, Forooghian F, Meyerle C (2013) Central serous chorioretinopathy: update on pathophysiology and treatment. Surv Ophthalmol 58:103–126

45. Iacono P, Battaglia PM, Papayannis A, La Spina C, Varano M, Bandello F (2015) Acute central serous chorioretinopathy: a correlation study between fundus autofluorescence and spectral-domain OCT. Graefes Arch Clin Exp Ophthalmol 253:1889–1897

46. Imamura Y, Fujiwara T, Spaide RF (2011) Fundus autofluorescence and visual acuity in central serous chorioretinopathy. Ophthalmology 118:700–705

47. Pang CE, Shah VP, Sarraf D, Freund KB (2014) Ultra-widefield imaging with autofluorescence and indocyanine green angiography in central serous chorioretinopathy. Am J Ophthalmol 158(362–371):e2

48. Reznicek L, Seidensticker F, Stumpf C, Kampik A, Thurau S, Kernt M, Neubauer A (2014) Systematic analysis of wide-field fundus autofluorescence (FAF) imaging in posterior uveitis. Curr Eye Res 39:164–171

49. Heussen FM, Vasconcelos-Santos DV, Pappuru RR, Walsh AC, Rao NA, Sadda SR (2011) Ultra-wide-field green-light (532-nm) autofluorescence imaging in chronic Vogt-Koyanagi-Harada disease. Ophthalmic Surg Lasers Imaging 42:272–277

50. Mesquida M, Llorenc V, Fontenla JR, Navarro MJ, Adan A (2014) Use of ultra-wide-field retinal imaging in the management of active Behcet retinal vasculitis. Retina 34:2121–2127

51. Hashimoto H, Kishi S (2015) Ultra-wide-field fundus autofluorescence in multiple evanescent white dot syndrome. Am J Ophthalmol 159:698–706

52. Seidensticker F, Neubauer AS, Wasfy T, Stumpf C, Thurau SR, Kampik A, Kernt M (2011) Wide-field fundus autofluorescence corresponds to visual fields in chorioretinitis patients. Clin Ophthalmol 5:1667–1671

53. Oishi A, Oishi M, Ogino K, Morooka S, Yoshimura N (2016) Wide-field fundus autofluorescence for retinitis pigmentosa and cone/cone-rod dystrophy. Adv Exp Med Biol 854:307–313

54. Lorenz B, Wabbels B, Wegscheider E, Hamel CP, Drexler W, Preising MN (2004) Lack of fundus autofluorescence to 488 nanometers from childhood on in patients with early-onset severe retinal dystrophy associated with mutations in RPE65. Ophthalmology 111:1585–1594

55. Ogura S, Yasukawa T, Kato A, Usui H, Hirano Y, Yoshida M, Ogura Y (2014) Wide-field fundus autofluorescence imaging to evaluate retinal function in patients with retinitis pigmentosa. Am J Ophthalmol 158:1093–1098

56. Hariri AH, Gui W, Datoo O'Keefe GA, Ip MS, Sadda SR, Gorin MB (2018) Ultra-widefield fundus autofluorescence imaging of patients with retinitis pigmentosa: a standardized grading system in different genotypes. Ophthalmol Retina 2:735–745

57. Oishi M, Oishi A, Ogino K, Makiyama Y, Gotoh N, Kurimoto M, Yoshimura N (2014) Wide-field fundus autofluorescence abnormalities and visual function in patients with cone and cone-rod dystrophies. Invest Ophthalmol Vis Sci 55:3572–3577

58. Oishi A, Ogino K, Makiyama Y, Nakagawa S, Kurimoto M, Yoshimura N (2013) Wide-field fundus autofluorescence imaging of retinitis pigmentosa. Ophthalmology 120:1827–1834

59. Trichonas G, Traboulsi EI, Ehlers JP (2016) Correlation of ultra-widefield fundus autofluorescence patterns with the underlying genotype in retinal dystrophies and retinitis pigmentosa. Ophthalmic Genet. https://doi.org/10.1080/13816810.2016.1227450:1-5

60. Allikmets R (1997) A photoreceptor cell-specific ATP-binding transporter gene (ABCR) is mutated in recessive Stargardt macular dystrophy. Nat Genet 17:122

61. Kjellstrom U (2014) Association between genotype and phenotype in families with mutations in the ABCA4 gene. Mol Vis 20:89–104

62. Allikmets R, Shroyer NF, Singh N et al (1997) Mutation of the Stargardt disease gene (ABCR) in age-related macular degeneration. Science 277:1805–1807

63. Klufas MA, Tsui I, Sadda SR, Hosseini H, Schwartz SD (2017) Ultrawidefield autofluoresence in Abca4 stargardt disease. Retina. https://doi.org/10.1097/IAE.0000000000001567

64. Kumar V (2017) Insights into autofluorescence patterns in Stargardt macular dystrophy using ultra-wide-field imaging. Graefes Arch Clin Exp Ophthalmol. https://doi.org/10.1007/s00417-017-3736-4

65. Abalem MF, Otte B, Andrews C, Joltikov KA, Branham K, Fahim AT, Schlegel D, Qian CX, Heckenlively JR, Jayasundera T (2017) Peripheral visual fields in ABCA4 stargardt disease and correlation with disease extent on ultra-widefield fundus autofluorescence. Am J Ophthalmol 184:181–188

66. Shen LL, Sun M, Grossetta Nardini HK, Del Priore LV (2019) Natural history of autosomal recessive stargardt disease in untreated eyes: a systematic review and meta-analysis of study- and individual-level data. Ophthalmology. https://doi.org/10.1016/j.ophtha.2019.05.015

67. Nagiel A, Lalane RA, Sadda SR, Schwartz SD (2016) Ultra-widefield fundus imaging: a review of clinical applications and future trends. Retina 36:660–678

68. Bell DJ, Wilson MW (2004) Choroidal melanoma: natural history and management options. Cancer Control 11:296–303

69. Albert DM, Robinson NL, Fulton AB et al (1980) Epidemikological investigation of increased incidence of choroidal melanoma in a single population of chemical workers. Int Ophthalmol Clin 20:71–92

70. Kernt M, Schaller UC, Stumpf C, Ulbig MW, Kampik A, Neubauer AS (2010) Choroidal pigmented lesions imaged by ultra-wide-field scanning laser ophthalmoscopy with two laser wavelengths (Optomap). Clin Ophthalmol 4:829–836

71. Reznicek L, Stumpf C, Seidensticker F, Kampik A, Neubauer AS, Kernt M (2014) Role of wide-field autofluorescence imaging and scanning laser ophthalmoscopy in differentiation of choroidal pigmented lesions. Int J Ophthalmol 7:697–703

72. Shields JA (1978) Melanocytoma of the optic nerve head: a review. Int Ophthalmol 1:31–37

73. Krohn J, Kjersem B (2011) Stereo fundus photography in the diagnosis of optic disc melanocytoma. Acta Ophthalmol 89:e533–e534

74. Arroyo JG, Yang L, Bula D, Chen DF (2005) Photoreceptor apoptosis in human retinal detachment. Am J Ophthalmol 139:605–610

75. Meyerle CB, Smith RT, Barbazetto IA, Yannuzzi LA (2007) Autofluorescence of basal laminar drusen. Retina 27:1101–1106

76. Albertus DL, Schachar IH, Zahid S, Elner VM, Demirci H, Jayasundera T (2013) Autofluorescence quantification of benign and malignant choroidal nevomelanocytic tumors. JAMA Ophthalmol 131:1004–1008

77. Salvanos P, Utheim TP, Moe MC, Eide N, Bragadomicronttir R (2015) Autofluorescence imaging in the differential diagnosis of optic disc melanocytoma. Acta Ophthalmol 93:476–480

78. Kadonosono K, Itoh N, Uchio E, Nakamura S, Ohno S (2000) Staining of internal limiting membrane in macular hole surgery. Arch Ophthalmol 118:1116–1118

79. Eckardt C, Eckert T, Eckardt U, Porkert U, Gesser C (2008) Macular hole surgery with air tamponade and optical coherence tomography-based duration of face-down positioning. Retina 28:1087–1096

80. Ciardella AP, Lee GC, Langton K, Sparrow J, Chang S (2004) Autofluorescence as a novel approach to diagnosing macular holes. Am J Ophthalmol 137:956–959

81. Shiragami C, Shiraga F, Nitta E, Fukuda K, Yamaji H (2012) Correlation of increased fundus autofluorescence signals at closed macula with visual prognosis after successful macular hole surgery. Retina 32:281–288

82. Nakao S, Arita R, Sato Y et al (2016) Wide-field laser ophthalmoscopy for imaging of gas-filled eyes after macular hole surgery. Clin Ophthalmol 10:1623–1630

83. Cook B, Lewis GP, Fisher SK, Adler R (1995) Apoptotic photoreceptor degeneration in experimental retinal detachment. Invest Ophthalmol Vis Sci 36:990–996

84. Hagimura N, Iida T, Suto K, Kishi S (2002) Persistent foveal retinal detachment after successful rhegmatogenous retinal detachment surgery. Am J Ophthalmol 133:516–520

85. Heimann H, Zou X, Jandeck C et al (2006) Primary vitrectomy for rhegmatogenous retinal detachment: an analysis of 512 cases. Graefes Arch Clin Exp Ophthalmol 244:69–78

86. Witmer MT, Cho M, Favarone G, Chan RV, D'Amico DJ, Kiss S (2012) Ultra-wide-field autofluorescence imaging in non-traumatic rhegmatogenous retinal detachment. Eye (Lond) 26:1209–1216

87. Salvanos P, Navaratnam J, Ma J, Bragadottir R, Moe MC (2013) Ultra-widefield autofluorescence imaging in the evaluation of scleral buckling surgery for retinal detachment. Retina 33:1421–1427

88. Singer M, Sagong M, van Hemert J, Kuehlewein L, Bell D, Sadda SR (2016) Ultra-widefield imaging of the peripheral retinal vasculature in normal subjects. Ophthalmology 123:1053–1059